2024 IEEE International Conference on Robotics and Automation (ICRA 2024)
May 13-17, 2024. Yokohama, Japan

Enhancing the Tracking Performance of Passivity-based High-Frequency Robot Cloud Control

Fabian Jakob, Xiao Chen, Hamid Sadeghian and Sami Haddadin

***Abstract*— This paper addresses the migration of high-frequency robot controllers to remote computing services, which are connected via a communication channel prone to delays and packet loss. The stability of the networked system is guaranteed by ensuring passivity of each subcomponent in the interconnection, as well as the Time-Domain-Passivity-Approach (TDPA) for the communication channel. We reduce conservatism of the TDPA using the model knowledge on both sides of the communication system to identify passivity excesses. This is further used to avoid over-dissipation of energy in the passivity controller by augmentation of a tolerable passivity-shortage. Tracking offsets are eliminated with a position drift compensation algorithm, for which convergence guarantees are provided. The experimental validation of the results conducted on a 7-DoF Franka Research 3 robot demonstrates a substantial enhancement in tracking performance due to the proposed modifications, particularly in scenarios with high communication delays.**

I. Introduction

Cloud robotics has emerged as a promising paradigm for enabling resource-intensive robotic tasks by offloading computation to remote servers. The use of Cloud and Edge-Cloud services have already been studied and exploited for computationally heavy use cases like Motion Planning [1], Image Processing in Visual Servoing [2] or Constrained Optimization [3]. The advantages are obvious, as large computation centers back boning the cloud offer almost unlimited amounts of computational power, allowing for reduced robot hardware requirements and increased modularity. However, all the aforementioned literature rely on low-level torque controller implemented on the robot realizing the computed cloud commands. Our previous work [4] presents a pioneering approach to also relocate the low-level high-frequency controller to the edge-cloud. This approach exploits the cloud potential to an even bigger extent, and moves towards a paradigm of separated hardware and software, allowing for remote monitoring/maintenance and easy system integration, with controller updates and upgrades being independent from extensive hardware modifications.

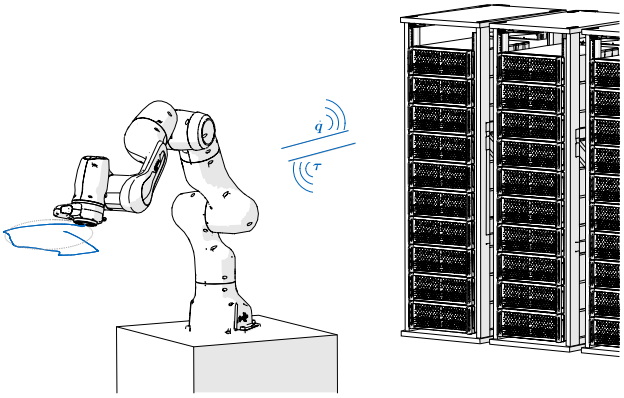

Fig. 1: Concept of relocating robot controller to the cloud.

However, networks and communication channels impose problems like delay or packet loss, which can be especially harmful in high-frequency control feedbacks, leading to potential instability. The previous work [4] utilizes the concept of passivity and implements the popular Time Domain Passivity Approach (TDPA) [5] to ensure stability of the whole network by passifying the communication channel with a respective passivity observer/controller (PO/PC). Whereas this approach is sufficient to stabilize the control interconnection, the control performance in terms of trajectory tracking is still shown to be poor for increasing delay and therefore, harms the applicability of this framework. Performance limitations resulting from the TDPA are known and already well studied in literature in the context of robot teleoperation. Results were conservatism reducing techniques [6], improved transparency [7] and position drift compensation algorithms [8, 9]. However, those methods are rather general and assume interaction with unknown human operators. The special case of cloud control on the other hand allows to exploit the knowledge of deterministic controller models on the remote side. Concepts like passivity-shortage can be introduced to characterize systems more precisely [10].

This paper aims at extending our previous work, focusing especially on the influence of the TDPA on the tracking performance in the context of the cloud control framework. The passivity analysis is employed as foundation of the presented theories. The interaction of network components is analyzed more coherently within the framework of passivity-shortages. The main contribution is the extension of the structure with a fairly easy implementable position drift com-

Authors are with the Munich Institute of Robotics and Machine Intelligence, Technical University of Munich, Munich, Germany and also with the Centre for Tactile Internet with Human-in-the-Loop (CeTI). {fabian.jakob, xiaoyu.chen, hamid.sadeghian, haddadin}@tum.de. H. Sadeghian also has an affiliation with University of Isfahan, 8174673441 Isfahan, Iran. The authors gratefully acknowledge the financial support by the Federal Ministry of Education and Research of Germany in the programme of "Souverän. Digital. Vernetzt.", Joint project 6G-life, project identification number: 16KISK002; the Cluster of Excellence "Centre for Tactile Internet with Human-in-the-Loop" (CeTI) funded by the German Research Foundation, Project ID 390696704; the funding of the Lighthouse Initiative Geriatronics by LongLeif GaPa gGmbH (Project Y) and the euROBIN and ReconCycle project, both funded by the European Union's Horizon 2020 Europe Framework Programme under grant agreement No 101070596 and 871352, respectively. Note that Sami Haddadin had a potential conflict of interest as shareholder of Franka Robotics (former Franka Emika) GmbH.

pensation algorithm with a convergence analysis. Moreover, a new method to reduce the conservatism of the TDPA by exploiting known model-based *passivity excesses* on both sides of the communication channel is proposed. Experimental results obtained from the implementation on a real robot validate the functionality of the approaches and therefore, make the whole framework more intriguing for industrial application.

This work is organized as follows. The next section introduce the theoretical foundations and preliminaries. Section III elaborates the framework introduced in [4] and addresses current limitations. Section IV introduces the proposed modifications and the mathematical analysis therewith, which are validated experimentally in Section V. Conclusions and future work are discussed in Section VI.

II. Preliminaries

A. Robot Model

In the scope of this work, general open-chain n-Degree-of-Freedom (DoF) rigid-body robots with joint angles $\boldsymbol{q} \in \mathbb{R}^n$ are considered. The robot joints follow the dynamics

$$\boldsymbol{M}(\boldsymbol{q})\ddot{\boldsymbol{q}} + \boldsymbol{C}(\boldsymbol{q},\dot{\boldsymbol{q}})\dot{\boldsymbol{q}} + \boldsymbol{D}\dot{\boldsymbol{q}} + \boldsymbol{g}(\boldsymbol{q}) = \boldsymbol{\tau} + \boldsymbol{\tau}_{\text{ext}} + \boldsymbol{\tau}_g, \quad (1)$$

where $\boldsymbol{M}, \boldsymbol{C}, \boldsymbol{D} \in \mathbb{R}^{n\times n}$, denote the inertia, Coriolis and damping matrices, respectively, and $\boldsymbol{g}(\boldsymbol{q})$ are the generalized gravitational forces acting on the joints. The robot is subject to the actuated controller and gravity compensation torques $\boldsymbol{\tau}$ and $\boldsymbol{\tau}_g$, respectively, and generalized external torques $\boldsymbol{\tau}_{\text{ext}}$. As most commercial lightweight robots are gravity compensated via respective, on-board firmware, this work considers the rewritten equations of motion

$$\boldsymbol{M}(\boldsymbol{q})\ddot{\boldsymbol{q}} + \boldsymbol{C}(\boldsymbol{q},\dot{\boldsymbol{q}})\dot{\boldsymbol{q}} + \boldsymbol{D}\dot{\boldsymbol{q}} = \boldsymbol{\tau} + \boldsymbol{\tau}_{\text{ext}}. \quad (2)$$

Thus, the relocation of the gravity compensation will explicitly not be regarded.

B. Passivity-based Control

The fundamental framework used to show stability with the cloud controller and communication channel is the concept of passivity. A general input/output (I/O) mapping $\Sigma : \boldsymbol{u} \mapsto \boldsymbol{y}$ is said to be passive, if there exists a constant $\gamma \in \mathbb{R}$, s.t. for all $T > 0$

$$\int_0^T \boldsymbol{u}(t)^T \boldsymbol{y}(t)\,\mathrm{d}t \geq -\gamma \quad (3)$$

for all admissable $\boldsymbol{u}$. For state space systems with state $\boldsymbol{x}$, (3) is equivalent to the existence of a positive semi-definite storage function $S(\boldsymbol{x}) \geq 0$, s.t. $\dot{S}(\boldsymbol{x}(t)) \leq \boldsymbol{u}(t)^T\boldsymbol{y}(t)$ [11]. A main exploitation of the passivity property in control design is the feedback theorem of passive systems, which states that the negative feedback interconnection of two systems Σ_1 and Σ_2 as depicted in Fig. 2 will be stable (and also passive w.r.t to external signals), if each system is passive w.r.t. it's respective I/O pair $(\boldsymbol{u}_i, \boldsymbol{y}_i)$, $i = 1, 2$ [11, 12]. The feedback theorem is especially exploited in the control in robotic systems, as a robot following (2) is known to be passive w.r.t. $(\dot{\boldsymbol{q}}, \boldsymbol{\tau} + \boldsymbol{\tau}_{\text{ext}})$ with storage function $S = \frac{1}{2}\dot{\boldsymbol{q}}^T\boldsymbol{M}(\boldsymbol{q})\dot{\boldsymbol{q}}$ [13]. A common assumption in literature is to assume the environment, e.g. a human or an obstacle, to be passive w.r.t $(\dot{\boldsymbol{q}}, -\boldsymbol{\tau}_{\text{ext}})$, e.g. in [14, 15]. Thus, to achieve a stable robot control, it is sufficient to the controller to be passive w.r.t. $(-\dot{\boldsymbol{q}}, \boldsymbol{\tau})$.

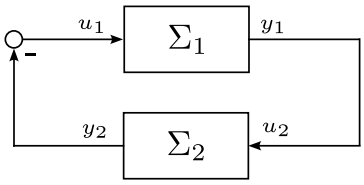

Fig. 2: Illustration of the feedback theorem for passive systems. If system Σ_1 is passive w.r.t $(\boldsymbol{u}_1, \boldsymbol{y}_1)$ and Σ_2 w.r.t $(\boldsymbol{u}_2, \boldsymbol{y}_2)$, then the shown interconnection is stable.

The theorem can even be extended for passivity-excessive, or respectively, passivity-short systems. We define an *excess* of passivity as

$$\int_0^T \left(\boldsymbol{u}(t)^T\boldsymbol{y}(t) - \|\boldsymbol{y}(t)\|^2_{\boldsymbol{Q}} - \|\boldsymbol{u}(t)\|^2_{\boldsymbol{R}}\right)\,\mathrm{d}t \geq -\gamma, \quad (4)$$

with some real symmetric matrices $\boldsymbol{Q}, \boldsymbol{R} \succeq \boldsymbol{0}$, called passivity indices. Analogously, define a *shortage* for $\boldsymbol{Q}, \boldsymbol{R} \preceq \boldsymbol{0}$. The generalized theorem states, that if both systems satisfy (4) with their respective $\boldsymbol{Q}_i, \boldsymbol{R}_i$, the interconnection is stable if[1] [11]

$$\boldsymbol{R}_1 + \boldsymbol{Q}_2 \succeq \boldsymbol{0}, \qquad \boldsymbol{R}_2 + \boldsymbol{Q}_1 \succeq \boldsymbol{0}. \quad (5)$$

Note, that the definitions (3, 4) and theorems analogously translate to time-discrete systems by taking the sum over all samples $\boldsymbol{u}_k, \boldsymbol{y}_k$, $k = 0, ..., T/t_s$ instead of the integral, whereas t_s is the sampling time of the discretized system [14].

C. Time-Domain Passivity Approach

In our cloud control framework, the robot is not directly connected to a controller, as a communication system arises in between. The TDPA is a discrete-time framework to enforce the passivity of arbitrary two-port communication network with generalized power pairs $(\boldsymbol{v}_1, \boldsymbol{f}_1)$ and $(\boldsymbol{v}_2, \boldsymbol{f}_2)$. Assume the network sends the velocity from port 1 to port 2 and the forces in the other direction, each with time-varying time delay, such that $\boldsymbol{v}_{2,k} = \boldsymbol{v}_{1,k-d_1}$ and $\boldsymbol{f}_{1,k} = \boldsymbol{f}_{2,k-d_2}$ for some $d_1, d_2 \in \mathbb{N}_0$. The TDPA enforces

$$t_s \sum_{k=0}^{n} \left(\boldsymbol{v}_{1,k}^T\hat{\boldsymbol{f}}_{1,k} + \hat{\boldsymbol{v}}_{2,k}^T\boldsymbol{f}_{2,k}\right) \geq -E(0), \;\; \forall n \geq 0 \quad (6)$$

with n being a discrete time-step, by adapting the respective transmitted effort variable with

$$\hat{\boldsymbol{f}}_{1,k} = \boldsymbol{f}_{1,k} + \alpha_k\,\boldsymbol{v}_{1,k}, \quad (7a)$$

$$\hat{\boldsymbol{v}}_{2,k} = \boldsymbol{v}_{2,k} + \beta_k\,\boldsymbol{f}_{2,k}. \quad (7b)$$

Eq. (7) is called *Passivity Controller* (PC) and damps the transmitted values if the delay/package loss endangers

[1]Note, that in it's original formulation in [11] the indices are assumed to have the structure $\boldsymbol{Q}_i = \delta_i\boldsymbol{I}$ and $\boldsymbol{R}_i = \epsilon_i\boldsymbol{I}$ for some $\delta_i, \epsilon_i \in \mathbb{R}$. However, the stability proof applies analogously for dense matrices *mutatis mutandis*.

passivity. W.l.o.g. set the initially stored energy in the system $E(0) = 0$. The dampings α and β are chosen according to a *Passivity Observer* (PO), which tracks the energy balance at each port $i = \{1, 2\}$ by observing the I/O power flow

$$p_i^{\text{in}} = \begin{cases} p_i & \text{, if } p_i > 0 \\ 0 & \text{, else,} \end{cases} \tag{8a}$$

$$p_i^{\text{out}} = \begin{cases} -p_i & \text{, if } p_i < 0 \\ 0 & \text{, else.} \end{cases} \tag{8b}$$

with $p_i = \boldsymbol{v}_i^T \boldsymbol{f}_i$. Obviously, $p_i = p_i^{\text{in}} - p_i^{\text{out}}$ and thus, the observed energy becomes

$$\begin{aligned} E_k^{\text{ob}} &= t_s \sum_{j=0}^{k} \left(\boldsymbol{v}_{1,j}^T \hat{\boldsymbol{f}}_{1,j} + \hat{\boldsymbol{v}}_{2,j}^T \boldsymbol{f}_{2,j} \right) \\ &= E_{1,k}^{\text{in}} - E_{1,k}^{\text{out}} + E_{1,k}^{\text{diss}} + E_{2,k}^{\text{in}} - E_{2,k}^{\text{out}} + E_{2,k}^{\text{diss}}, \end{aligned} \tag{9}$$

with

$$E_{i,k}^{\text{in}} = t_s \sum_{j=0}^{k} p_{i,j}^{\text{in}}, \qquad E_{i,k}^{\text{out}} = t_s \sum_{j=0}^{k} p_{i,j}^{\text{out}}, \tag{10}$$

$$E_{1,k}^{\text{diss}} = t_s \sum_{j=0}^{k} \alpha_j \|\boldsymbol{v}_{1,j}\|^2, \quad E_{2,k}^{\text{diss}} = t_s \sum_{j=0}^{k} \beta_j \|\boldsymbol{f}_{2,j}\|^2 \tag{11}$$

Note that E_i^{in} is a monotonously increasing function, such that a sufficient condition for $E_k^{\text{ob}} \geq 0$ is

$$E_{2,k}^{\text{in}} \geq E_{2,k-d_2}^{\text{in}} \geq E_{1,k}^{\text{out}} - E_{1,k}^{\text{diss}} \tag{12a}$$

$$E_{1,k}^{\text{in}} \geq E_{1,k-d_1}^{\text{in}} \geq E_{2,k}^{\text{out}} - E_{2,k}^{\text{diss}}. \tag{12b}$$

The advantage of the formulation (12) is that both ports now can evaluate a passivity condition even though their mutual information is separated by the delayed/lossy communication. The choice of α and β can then be determined by

$$\alpha_k = \begin{cases} \frac{-W_{1,k}}{t_s \|\boldsymbol{v}_{1,k}\|^2} & \text{, if } W_{1,k} < 0,\ \|\boldsymbol{v}_{1,k}\| \neq 0 \\ 0 & \text{, else,} \end{cases} \tag{13}$$

$$\beta_k = \begin{cases} \frac{-W_{2,k}}{t_s \|\boldsymbol{f}_{2,k}\|^2} & \text{, if } W_{2,k} < 0,\ \|\boldsymbol{f}_{2,k}\| \neq 0 \\ 0 & \text{, else,} \end{cases} \tag{14}$$

with the port's energy balances

$$W_{1,k} = E_{2,k-d_2}^{\text{in}} - E_{1,k}^{\text{out}} + E_{1,k-1}^{\text{diss}}, \tag{15a}$$

$$W_{2,k} = E_{1,k-d_1}^{\text{in}} - E_{2,k}^{\text{out}} + E_{2,k-1}^{\text{diss}}. \tag{15b}$$

This particular choice dissipates the exact necessary amount to render $W_{i,k}$ zero as soon as it would become negative. This enforces (12), which implies $E_k^{\text{ob}} \geq 0$ and thus, the two-port system is passive w.r.t $([\boldsymbol{v}_1\ \hat{\boldsymbol{v}}_2]^T, [\hat{\boldsymbol{f}}_1\ \boldsymbol{f}_2]^T)$.

III. The Remote Robot Control Framework

The principle of the remote control framework introduced in [4] can be illustrated with Fig. 3. The framework analyzes each robot, environment, communication channel and controller as an individual passive system. The whole interconnection as a result of nested feedback interconnections of passive systems will then be stable.

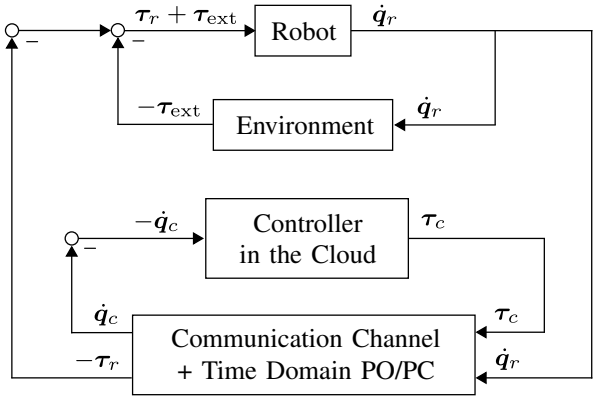

Fig. 3: Illustration of the Controller-in-the-Cloud Framework. Each component is analysed as subsystem, and interconnected with the other subsystems in feedback loops. The communication channel is considered a two-port system, which uses a passivity observer/controller to be rendered passive.

A. Passivity of the High-Frequency Controller

The controller is located in a feedback loop with the second port of the communication channel. We denote its input and output respectively as $\dot{\boldsymbol{q}}_c$ and $\boldsymbol{\tau}_c$. For the sake of this work, consider as high-frequency cloud controller a simple Cartesian PD controller

$$\boldsymbol{\tau}_c = \boldsymbol{J}(\boldsymbol{q}_c)^T (\boldsymbol{K}_p\, \tilde{\boldsymbol{x}} + \boldsymbol{K}_d\, \dot{\tilde{\boldsymbol{x}}}) \tag{16}$$

with the task space error $\tilde{\boldsymbol{x}} = \boldsymbol{x}_{\text{ref}} - \boldsymbol{x}_c$ and positive definite gain matrices $\boldsymbol{K}_p, \boldsymbol{K}_d$. The passivity of this controller w.r.t $(-\dot{\boldsymbol{q}}_c, \boldsymbol{\tau}_c)$ can be shown straightforward using the positive semi-definite storage function $S = \frac{1}{2}\tilde{\boldsymbol{x}}^T \boldsymbol{K}_p \tilde{\boldsymbol{x}}$ [16]. Essentially, the controller can be extended by arbitrary passive components. Our previous work [4] used a Unified Force Impedance Controller (UFIC) for a simultaneous trajectory and force tracking, which can also be shown to be passive w.r.t. the same power pair [16] by augmenting an virtual energy tank. However, the authors would like to highlight that through the use of the TDPA, the controller can have any arbitrary implementation that behaves passive w.r.t $(-\dot{\boldsymbol{q}}_c, \boldsymbol{\tau}_c)$ *or* $(\dot{\boldsymbol{q}}_c, \boldsymbol{\tau}_c)$. The reason is that the controller is not in direct interconnection with the robot anymore but with the communication channel, whose power balance behaviour can be *designed* with the PO/PC by the choice of power pair. In example, if the controller is passive w.r.t. $(-\dot{\boldsymbol{q}}_c, \boldsymbol{\tau}_c)$, the power pair of the admittance PC is then chosen as $(\hat{\boldsymbol{v}}_2, \boldsymbol{f}_2) := (\dot{\boldsymbol{q}}_c, \boldsymbol{\tau}_c)$ and *vice versa*.

B. Passivation of the Communication Channel

We denote the transmitted robot velocity measurements and transmitted torques as $\dot{\boldsymbol{q}}_{r,d_1}(t) := \dot{\boldsymbol{q}}_r(t - d_1(t))$ and $\boldsymbol{\tau}_{c,d_2}(t) := \boldsymbol{\tau}_c(t - d_2(t))$, respectively, with some time-varying delays $d_1(t), d_2(t)$. Analogously, define for the time-discrete framework $\dot{\boldsymbol{q}}_{r,k-d_1} := \dot{\boldsymbol{q}}_{r,d_1}(kt_s)$ and $\boldsymbol{\tau}_{c,k-d_2} := \boldsymbol{\tau}_{c,d_2}(kt_s)$. W.l.o.g. package losses are modelled within d_1 and d_2.

The power variables for the TDPA implementation are chosen with power signs opposite to robot/control, such that according to section II-A and III-A they are selected as

$(\boldsymbol{v}_1, \hat{\boldsymbol{f}}_1) := (\dot{\boldsymbol{q}}_r, -\boldsymbol{\tau}_r)$ and $(\hat{v}_2, \boldsymbol{f}_2) := (\dot{\boldsymbol{q}}_c, \boldsymbol{\tau}_c)$, see Fig. 3. The PC law therefore becomes

$$\boldsymbol{\tau}_{r,k} = \boldsymbol{\tau}_{c,k-d_2} - \alpha_k \dot{\boldsymbol{q}}_{r,k} \tag{17a}$$

$$\dot{\boldsymbol{q}}_{c,k} = \dot{\boldsymbol{q}}_{r,k-d_1} + \beta_k \boldsymbol{\tau}_{c,k-1}. \tag{17b}$$

Note the index shift of $\boldsymbol{\tau}_{c,k-1}$ to avoid an algebraic loop.

For the sake of trajectory tracking however, note that unlike most common robotic control literature, the controller has no access to the measured joint angles $\boldsymbol{q}_r$. Although one could naively use the delayed joint angles $\boldsymbol{q}_{r,d_1}$, the passivity proof of the controller is only valid using $\boldsymbol{q}_c$. Thus, the implementation requires a prior numerical integration of the transmitted cloud velocities $\dot{\boldsymbol{q}}_c$. For sufficiently small sample times t_s, the integration error is neglectable. However, as the PC modifies the transmitted velocities, a position drift

$$\Delta \boldsymbol{q}_k := t_s \sum_{j=d}^{k} (\dot{\boldsymbol{q}}_{c,j} - \dot{\boldsymbol{q}}_{r,j-d_1}) \tag{18}$$

arises, caused by the admittance PC (17b). Obviously, such a position drift is disastrous for any kind of trajectory tracking problem, as the performance is limited to the reference tracking of the cloud position $\boldsymbol{x}_c$, which deviates from the real robot position $\boldsymbol{x}_r$ when delay arises. In the worst case that leads to stationary offsets and dynamic drifts. Section IV introduces two modifications, that both will address this issue.

IV. Proposed Tracking Improvements

After introducing the framework and the respective remaining issues, this section proposes modifications together with the mathematical analysis to improve the framework with regard to the tracking performance.

A. Position Drift Compensation

Consider the defined position drift $\Delta \boldsymbol{q}_k$ from eq. (18) and obtain the error dynamics

$$\Delta \boldsymbol{q}_k = t_s \sum_{j=d_1}^{k} \underbrace{(\dot{\boldsymbol{q}}_{c,j} - \dot{\boldsymbol{q}}_{r,j-d_1})}_{=\beta_j \boldsymbol{\tau}_{c,j-1}} = \Delta \boldsymbol{q}_{k-1} + t_s\, \beta_k \boldsymbol{\tau}_{c,k-1}. \tag{19}$$

Observe, that as long as the controller torque $\boldsymbol{\tau}_c$ is not opposing the position error direction, the drift will be monotonously increasing at every time instance. To achieve a stable error dynamics, we introduce an additive feedback of the position drift to the received velocities

$$\dot{\tilde{\boldsymbol{q}}}_{r,k-d_1} := \dot{\boldsymbol{q}}_{r,k-d_1} - \boldsymbol{K}_{\mathrm{pos}} \Delta \boldsymbol{q}_{k-1}. \tag{20}$$

Note, that the transmitted velocities now get modified twice: once by the position drift compensation and once by the PC. The corresponding extended block diagram structure is given in Fig. 4. However, as (20) is also used as input to the PO, passivity remains untouched. Formulating the new error dynamics then, we have

$$\Delta \boldsymbol{q}_k = (\boldsymbol{I} - t_s \boldsymbol{K}_{\mathrm{pos}})\, \Delta \boldsymbol{q}_{k-1} + t_s\, \beta_k \boldsymbol{\tau}_{c,k-1}. \tag{21}$$

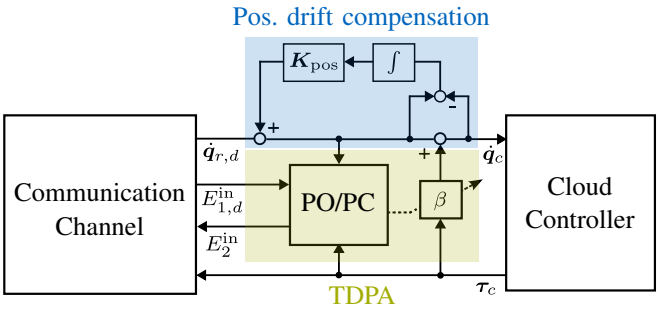

Fig. 4: Extended TDPA structure on the cloud side with the proposed position drift compensation.

Therefore, if and only if the matrix $(\boldsymbol{I} - t_s \boldsymbol{K}_{\mathrm{pos}})$ is Schur, i.e. has maximum absolute value smaller than one, the error dynamics will be input-to-state stable w.r.t. the disturbance $\beta_k \boldsymbol{\tau}_{c,k-1}$ and exponentially converging to zero for $\beta_k = 0$ [17]. Note, that this is a necessary and sufficient design condition for a general feedback matrix $\boldsymbol{K}_{\mathrm{pos}}$, leaving also the possibility e.g. for different weighting of joint errors. Note also, that we interpret the summation of velocity difference as first order integration method, whereas also all other numerical integration methods would be feasible.

B. Passivity-Shortage Augmentation

Intuitively, the PC can be regarded as energy dissipation through damping of the respective effort. On the other hand, both controller and robot already have dissipative character, which is not considered within the TDPA energy balances. Over-conservative damping might degrade the control performance unnecessarily. Recall the definitions of passivity/excess shortages from section II-B. If for both robot and controller some passivity excesses can be identified, the passivity theorem allows the PO/PC to permit some passivity shortage to reduce the overall conservatism. We will show, that such excesses are direct causes of dissipative character on both sides.

Consider the PD controller (16) and the storage function $S_c = \frac{1}{2} \tilde{\boldsymbol{x}}^T \boldsymbol{K}_p \tilde{\boldsymbol{x}}$. W.l.o.g. assume $\dot{\boldsymbol{x}}_{\mathrm{ref}} = 0$, and obtain the derivative

$$\begin{aligned} \dot{S}_c &\overset{(\dots)}{=} -\dot{\boldsymbol{q}}_c^T \boldsymbol{\tau}_c - \dot{\boldsymbol{x}}_c^T \boldsymbol{K}_d \dot{\boldsymbol{x}}_c \\ &= -\dot{\boldsymbol{q}}_c^T \boldsymbol{\tau}_c - \underbrace{\dot{\boldsymbol{q}}_c^T \boldsymbol{J}^T(\boldsymbol{q}_c) \boldsymbol{K}_d \boldsymbol{J}(\boldsymbol{q}_c) \dot{\boldsymbol{q}}_c}_{=:\|\dot{\boldsymbol{q}}_c\|^2_{\boldsymbol{R}_1^c}}. \end{aligned} \tag{22}$$

Recalling definition (4), eq. (22) implies a passivity excess with index $\boldsymbol{R}_1^c = \boldsymbol{J}^T \boldsymbol{K}_d \boldsymbol{J} \succeq \boldsymbol{0}$. Likewise, consider robot (2) and the storage $S_r = \frac{1}{2} \dot{\boldsymbol{q}}_r^T \boldsymbol{M}(\boldsymbol{q}_r) \dot{\boldsymbol{q}}_r$. W.l.o.g. assume $\boldsymbol{\tau}_{\mathrm{ext}} = 0$ and obtain

$$\dot{S}_r \overset{(\dots)}{=} \dot{\boldsymbol{q}}_r^T \boldsymbol{\tau}_r - \underbrace{\dot{\boldsymbol{q}}_r^T \boldsymbol{D} \dot{\boldsymbol{q}}_r}_{=:\|\dot{\boldsymbol{q}}_r\|^2_{\boldsymbol{Q}_2^r}}, \tag{23}$$

which analogously implies a passivity excess with index $\boldsymbol{Q}_2^r = \boldsymbol{D} \succeq \boldsymbol{0}$. Conclusively, both sides of the communication channel allow for passivity shortage without endangering the stability of the interconnection. We call the passivity shortages of the TDPA on cloud and robot side $\boldsymbol{Q}_2^c$ and $\boldsymbol{R}_1^r$, respectively.

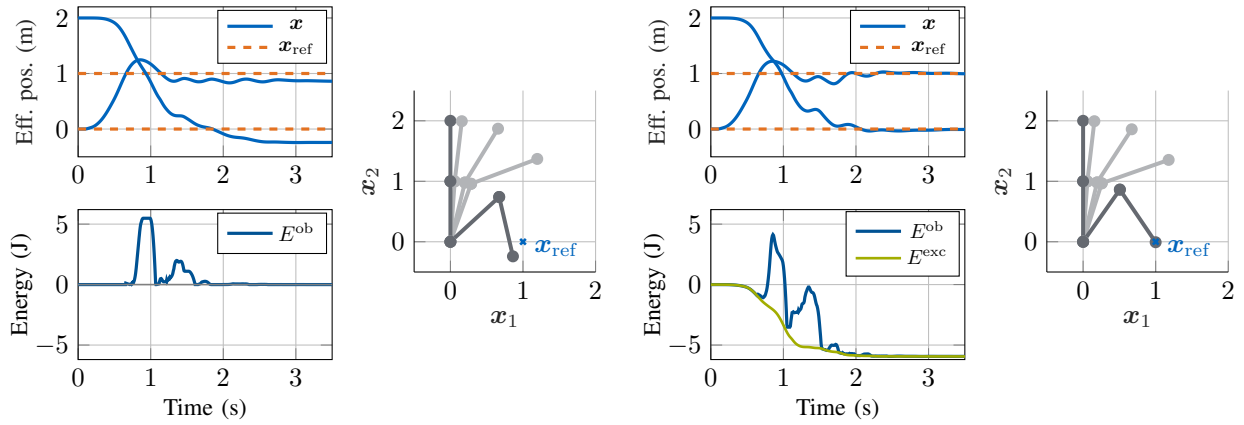

(a) Failed regulation without modifications due to position drift. The peak PC dampings were $\alpha_{\max} = 9.59 \cdot 10^3$, $\beta_{\max} = 0.37$.

(b) Successful regulation with modifications. The peak PC dampings were $\alpha_{\max} = 9.54 \cdot 10^3$, $\beta_{\max} = 0.02$.

Fig. 5: Illustrative comparison of the remote control framework, in (a) without and in (b) with proposed modifications, using a planar 2-DoF robot simulation model with modelled communication delay of 50 ms, $\boldsymbol{K}_{\text{pos}} = 2\boldsymbol{I}$ and $\eta = 0.9$.

To augment a shortage to the PO/PC, consider instead of (15) the modified energy balances

$$\hat{W}_{1,k} = W_{1,k} + t_s \sum_{j=1}^{k} \eta \|\dot{\boldsymbol{q}}_{r,j}\|^2_{\boldsymbol{Q}_2^r}, \tag{24a}$$

$$\hat{W}_{2,k} = W_{2,k} + t_s \sum_{j=1}^{k-1} \eta \|\dot{\boldsymbol{q}}_{c,j}\|^2_{\boldsymbol{R}_1^c}, \tag{24b}$$

with some $\eta > 0$ and let both PC enforce $\hat{W}_i > 0$. Then, $\hat{W}_{1,k} + \hat{W}_{2,k}$ provides a lower bound on the altered modified energy

$$\hat{E}^{\text{ob}} = t_s \sum \left(\hat{\boldsymbol{v}}_1^T \boldsymbol{f}_1 + \boldsymbol{v}_2^T \hat{\boldsymbol{f}}_2 + \eta \|\hat{\boldsymbol{v}}_1\|^2_{\boldsymbol{R}_1^c} + \eta \|\boldsymbol{v}_2\|^2_{\boldsymbol{Q}_2^r} \right). \tag{25}$$

Eq. (25) conforms to the time-discrete correspondence of (4). Therefore, modifications (24) achieves a passivity-shortage in the TDPA with $\boldsymbol{Q}_2^c = \eta \boldsymbol{R}_1^c$ and $\boldsymbol{R}_1^r = \eta \boldsymbol{Q}_2^r$. Recall the stability criteria $\boldsymbol{R}_1^r + \boldsymbol{Q}_2^r \succeq 0$ and $\boldsymbol{R}_2^c + \boldsymbol{Q}_1^c \succeq 0$. This allows to choose $\eta \in [0, 1]$ while still maintaining stability.

Remark: Note the index shift in the sum in (24b) to avoid an algebraic loop, as the computation of $\hat{W}_{2,k}$ would require $\dot{\boldsymbol{q}}_{c,k}$ and *vice versa*. However, as the summation is monotonously increasing, this does not affect the lower bound.

Note, that the choice of $\eta > 0$ renders $\hat{W}_i \geq W_i$. Therefore, the intervention of the PC will be generally reduced as $W_i > 0$ is replaced by the milder condition $\hat{W}_i > 0$. Therefore, the larger the passivity indices $\boldsymbol{R}_1^c, \boldsymbol{Q}_2^r$, the milder the PC will become. Note that $\boldsymbol{R}_1^c$ and $\boldsymbol{Q}_2^r$ are direct results of some damping in either the robot and the controller. Thus, the passivity excess can be interpreted as an amount of dissipated energy, that the PC has available as stability margin. The modification (24) conclusively reduces the conservatism of the whole TDPA. We highlight, that to the best of our knowledge, the use of passivity excesses as a result of model knowledge has not yet been exploited in TDPA literature.

C. Simulation example

The proposed modifications are illustrated with a simulation example in Fig. 5, where a simple 2-DoF planar robot should move to a reference point $\boldsymbol{x}_{\text{ref}}$ using a relocated cloud controller with modelled communication delay of 50 ms. Compare Fig. 5a without and Fig. 5b with both proposed modifications from sec. IV-A and IV-B, as visibly the position drift caused by the admittance PC can be compensated. Observe also the PO energy E^{ob}, which takes significantly lower values as it has an improved lower bound $E^{\text{exc}} := -t_s \sum \|\dot{\boldsymbol{q}}_c\|^2_{\boldsymbol{R}_1^c} + \|\dot{\boldsymbol{q}}_r\|^2_{\boldsymbol{Q}_2^r}$, leading to reduced PC dampings $\alpha_{\max}, \beta_{\max}$.

V. Experimental Evaluation

A. Experiment Setup

The proposed modifications are validated on a cloud control testbed, including a 7-DoF Franka Research 3 robot [18] and two Intel NUCs, whereas one sends commands to the robot with 1 kHz rate through the Franka Control Interface (FCI) and the other represents the cloud edge on which all control commands are computed. Both NUCs are connected through Ethernet cables and are transmitting data using the User Datagram Protocol (UDP). To emulate the characteristics of wireless communication channels, the open-source traffic control tool `tcgui` [19] is used to impose artificial delay

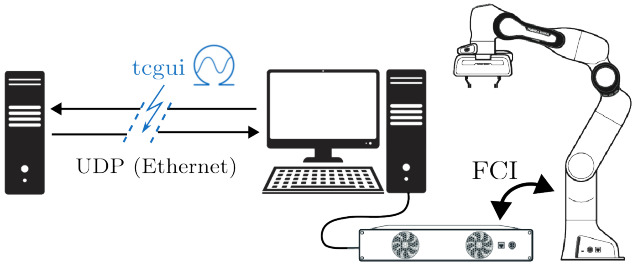

Fig. 6: Illustration of the cloud control testbed.

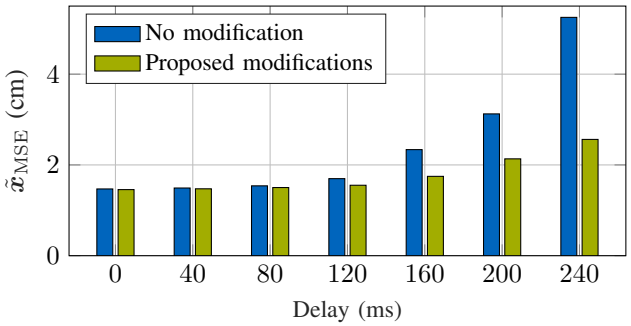

Fig. 7: Comparison of mean square tracking error for different communication round-trip delays of previous method and with modification.

with $\pm 5\%$ variation and 3% packet loss. The testbed is illustrated in Fig. 6.

The experiment is set up to follow a circular trajectory with radius of 10 cm with a period of 5 s while having surface contact with a table board. A PO/PC is implemented on each NUC for communication passivation. The cloud controller implements a PD controller with gains $\boldsymbol{K}_p = 500\boldsymbol{I}$ and $\boldsymbol{K}_d = 40\boldsymbol{I}$ and a position drift compensation gain of $\boldsymbol{K}_{\mathrm{pos}} = 5\boldsymbol{I}$. The shortage augmentation scaling are set to $\eta = 0.6$. The gains are tuned heuristically to trade-off bandwidth and oscillatory behaviour.

B. Results

The trajectory tracking experiment is repeated for several communication delays, ranging from 0 ms to 240 ms, each with and without modifications. The evolution of the mean square tracking error (MSE) $\tilde{\boldsymbol{x}}_{\mathrm{MSE}}$ distributed over all delays is given in Fig. 7. Observe that as expected, the tracking error grows with higher delays. However, the proposed modifications can visibly reduce the tracking error, especially in the range of high delays. This meets the expectation, as the TDPA influence rises with higher delays and thus, the modifications become more effective. For delays higher than 240 ms, the robot runs into firmware defined torque or velocity saturation limits. Except for 0 ms delay, all experiments would have been unstable without the implemented TDPA.

A detailed tracking plot, selectively chosen for the experiment with 160 ms, is given in Fig. 8. The plot shows the resulting robot trajectories in cartesian space, whereas both the real robot position $\boldsymbol{x}_r$ and the virtual cloud position $\boldsymbol{x}_c$ are plotted. As expected, a position drift error $\Delta\dot{\boldsymbol{q}}$ arises without modifications in 8a, as the blue and red deviate from each other. Notably, the cloud position evolves into the table, which causes the robot to slightly jump on the surface. On the other hand, enabling the modifications eliminates such errors and leads to overall better reference tracking, see 8b. Compare also the magnitudes of the PC dampings α and β, which can be reduced significantly, confirming the effect of the improved energy bound resulting from the shortage augmentation.

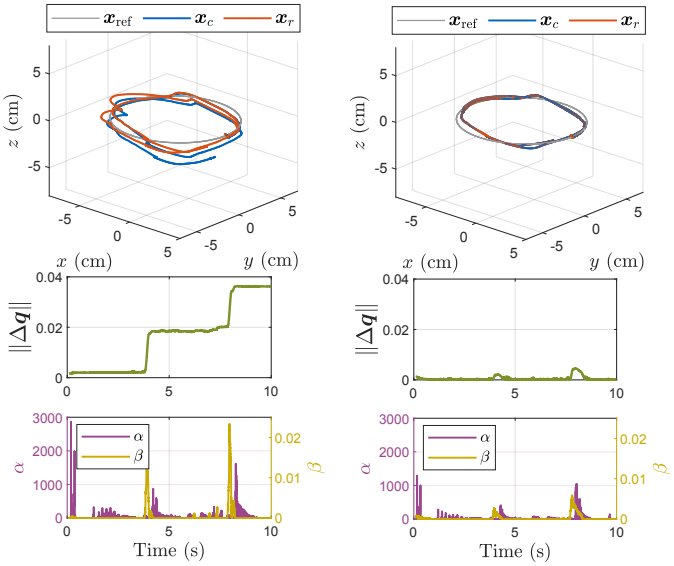

(a) Without modification. (b) With modifications.

Fig. 8: Comparison of the results with and without modification for round-trip delay of 160 ms.

VI. Conclusion

To conclude this paper, the given analysis shows that the tracking performance of cloud-based relocated high-frequency controller can be significantly improved. The results have been validated using a simple PD controller, however, extensions to more complex type of controllers is possible, as discussed. We proposed two modifications to enhance the use of the TDPA, a position drift compensation to eliminate deviation of real and virtual position, and a passivity-shortage augmentation to reduce the conservatism of the TDPA. Results have been validated in simulation and on a testbed with a real Franka Research 3 robot and artificially delayed communication channel, which both show the effect of the proposed modifications in terms of notably better tracking performance and lower PC intervention. Therefore, the whole framework becomes more attractive for applications and pushes to conduct more research in that field for the vision of fully relocated robot software.

Future work includes further extension of the framework, like the integration of force measurements in the TDPA framework to ensure stable force control. Additionally, one might address the safety issue of such a framework and discuss encryption necessities of the traffic flow. Finally, the extension to multi-robot collaborative cloud control will be investigated.

References

[1] V. Vonasek, R. Pěnička, A. Vick, and J. Krüger, "Robot control as a service - towards cloud-based motion planning and control for industrial robots," 07 2015.

[2] H. Wu, L. Lou, C.-C. Chen, S. Hirche, and K. Kuhnlenz, "Cloud-based networked visual servo control," *IEEE Transactions on Industrial Electronics*, vol. 60, no. 2, 2013.

[3] H. Zhu, M. Sharma, K. Pfeiffer, M. Mezzavilla, J. Shen, S. Rangan, and L. Righetti, "Enabling remote whole-body control with 5g edge computing," *CoRR*, vol. abs/2008.08243, 2020.

[4] X. Chen, H. Sadeghian, L. Chen, M. Tröbinger, A. Swirkir, A. Naceri, and S. Haddadin, "A passivity-based approach on relocating high-frequency robot controller to the edge cloud," in *2023 IEEE International Conference on Robotics and Automation (ICRA)*, 2023, pp. 5242–5248.

[5] J.-H. Ryu, J. Artigas, and C. Preusche, "A passive bilateral control scheme for a teleoperator with time-varying communication delay," *Mechatronics*, vol. 20, no. 7, 2010.

[6] M. Panzirsch, J.-H. Ryu, and M. Ferre, "Reducing the conservatism of the time domain passivity approach through consideration of energy reflection in delayed coupled network systems," *Mechatronics*, vol. 58, 2019.

[7] H. Singh, A. Jafari, and J.-H. Ryu, "Enhancing the force transparency of time domain passivity approach: Observer-based gradient controller," 05 2019, pp. 1583–1589.

[8] A. Coelho, H. Singh, T. Muskardin, R. Balachandran, and K. Kondak, "Smoother position-drift compensation for time domain passivity approach based teleoperation," *2018 IEEE/RSJ International Conference on Intelligent Robots and Systems (IROS)*, pp. 5525–5532, 2018.

[9] J. Artigas, J.-H. Ryu, and C. Preusche, "Position drift compensation in time domain passivity based teleoperation," in *2010 IEEE/RSJ International Conference on Intelligent Robots and Systems*, 2010, pp. 4250–4256.

[10] D. Babu Venkateswaran and Z. Qu, "Passivity-short bilateral teleoperation with communication delays," in *2018 IEEE International Conference on Systems, Man, and Cybernetics (SMC)*, 2018, pp. 1275–1281.

[11] H. K. Khalil, *Nonlinear systems; 3rd ed.* Upper Saddle River, NJ: Prentice-Hall, 2002, the book can be consulted by contacting: PH-AID: Wallet, Lionel. [Online]. Available: https://cds.cern.ch/record/1173048

[12] T. Hatanaka, N. Chopra, M. Fujita, and M. Spong, *Passivity-Based Control and Estimation in Networked Robotics*. Springer Publishing Company, Incorporated, 2015.

[13] B. Siciliano, L. Sciavicco, L. Villani, and G. Oriolo, *Robotics: Modelling, Planning and Control*. Springer Publishing Company, Incorporated, 2010.

[14] D. Lee and M. Spong, "Passive bilateral teleoperation with constant time delay," *IEEE Transactions on Robotics*, vol. 22, no. 2, pp. 269–281, 2006.

[15] N. Hogan, "Controlling impedance at the man/machine interface," in *Proceedings, 1989 International Conference on Robotics and Automation*, 1989, pp. 1626–1631 vol.3.

[16] C. Schindlbeck and S. Haddadin, "Unified passivity-based cartesian force/impedance control for rigid and flexible joint robots via task-energy tanks," in *2015 IEEE International Conference on Robotics and Automation (ICRA)*, 2015, pp. 440–447.

[17] Z.-P. Jiang and Y. Wang, "Input-to-state stability for discrete-time nonlinear systems," *Automatica*, vol. 37, no. 6, pp. 857–869, 2001. [Online]. Available: https://www.sciencedirect.com/science/article/pii/S0005109801000280

[18] S. Haddadin, S. Parusel, L. Johannsmeier, S. Golz, S. Gabl, F. Walch, M. Sabaghian, C. Jähne, L. Hausperger, and S. Haddadin, "The franka emika robot: A reference platform for robotics research and education," *IEEE Robotics & Automation Magazine*, vol. 29, pp. 2–20, 06 2022.

[19] B. Heß, C. Sieber, M. Hofbauer, and TUM LKN team, "tcgui: A lightweight Python-based Web-GUI for Linux traffic control," Jul. 2016. [Online]. Available: https://github.com/tum-lkn/tcgui